ISSN: 2277-9655
Impact Factor: 4.116
CODEN: IJESS7

IJESRT

INTERNATIONAL JOURNAL OF ENGINEERING SCIENCES & RESEARCH TECHNOLOGY

EQUILIBRIUM AND KINETIC STUDIES OF BIOSORPTION OF REACTIVE ORANGE 13 FROM AQUEOUS SOLUTION BY DEAD BIOMASS OF RHIZOPUS ARRHIZUS

Sukhada Saraf*, Varsha K. Vaidya
[*] The Institute of Science, 15, Madam Cama Road, Mumbai 400 032, Maharashtra, India

DOI: 10.5281/zenodo.160876

ABSTRACT

The equilibrium and kinetics of the biosorption of Reactive Orange 13from aqueous solution were investigated using dead biomass of Rhizopus arrhizus in a batch system. Biosorption equilibrium was established in about 180min. The sorption data obtained at pH 2.0 conformed well to the Langmuir isotherm model. The biosorption data of Reactive Orange 13 were analyzed using the pseudo-first order, the pseudo-second order, Elovich kinetics models as well as intra-particular rate diffusion and liquid film diffusion models. The pseudo-second-order equation was the most appropriate equation to predict the biosorption kinetics. The reusability of the biosorbent was tested in five consecutive adsorption–desorption cycles and the regeneration efficiency was above 95%. The XRD, BET, SEM and FITR analyses helped to elucidate the mechanism of biosorption. From the practical viewpoint, the abundant and inexpensive dead fungal biomass could be used as an effective, low cost and eco-friendly biosorbent for the removal of Reactive Orange 13from the aqueous solution.

KEYWORDS: Rhizopus arrhizus; Biosorption; Reactive Orange 13; Isotherms; Kinetics.

INTRODUCTION

Over 1 million tons of disperse, reactive and direct dyes are produced per year which are mainly used as textile dyes. In 2010, India produced ~200,000 tonnes of dyes. Of this, 50% were reactive dyes due to the availability of important raw materials like vinyl sulphone as well as their technical characteristics such as bright and water-fast colors, simple application techniques with low energy consumption. Globally, it has been estimated that 2% of the total dyes produced annually are discharged in effluents from manufacturing operations whilst 10 % of the total dyestuff used are discharged from textile and associated industries (Swamy, 1998;Walker et al.,2003). Textile industry is one of the most water- demanding industries worldwide and the textile industry effluent is rated as the most polluting among all the industrial sectors (Arslan et al., 2006).In general, the effluent is highly coloured with high biological oxygen demand (BOD) and chemical oxygen demand (COD), a high conductivity and alkalinity. The majority of the BOD is due to soluble, colourless organics such as emulsifiers, bleaches, soaps, oils, as well as dispersing, desizing, scouring, levelling and reducing agents, surfactants etc. (Zille, 2005; Swamy and Ramsay, 1999).

The release of coloured wastewater in the ecosystem is a prominent source of aesthetic pollution, eutrophication and perturbations in natural equilibrium of the aquatic environment (Aravind et al., 2010). Dyes, even at very low concentrations, reduce wastewater transparency and oxygen solubility and are often toxic, carcinogenic or mutagenic for various organisms (Mathur and Bhatnagar,2007). Textile dyes are designed to resist fading upon exposure to sweat, light, water, oxidizing agents and microbial attack. Various physico-chemical processes like electrokinetic coagulation, chemical precipitation, ion-exchange, ozonation, membrane filtration, photo-degradation etc. are of limited use due to different constraints such as costs, general applicability and production of the solid wastes (Zille, 2005; Murugesan, 2003). Unfavourable conditions found in the textile dyeing effluents are known to inhibit the conventional biological wastewater treatment processes. Moreover, various azo dyes have been shown to be anaerobically decolorized by the cleavage of the azo bond, resulting in the formation of potentially carcinogenic aromatic amines (Murugesan, 2003). Thus, no single solution has been satisfactory for remediating the broad diversity of textile wastes.

ISSN: 2277-9655
Impact Factor: 4.116
CODEN: IJESS7

Removal of the colour from the effluents is thus a major problem and implementation of tighter constraints on the discharges is forcing waste creators and managers to exploit new cost-effective technologies of wastewater treatment for environmental restoration (Ibrahim and Sani, 2014). Among all the wastewater treatments, the adsorption process has been recognized to be an effective and economical procedure for the dye removal from industrial effluent. Adsorption can handle large flow rates, producing a high-quality effluent that does not result in the formation of harmful substances. The commercial application of activated carbon, one of the most widely used adsorbents, is limited, due to its high cost, difficulty in regeneration, problems with regard to final disposal, inefficient adsorption of cationic dyes despite its good adsorption capacity (Erden et al., 2011; Russo et al., 2009;Skult, 2009). Hence, low-cost and readily available biosorbent materials with high adsorption capacities have gained increasing attention in reducing the adsorbent dose and minimizing the disposal problem (Chen et al., 2005).These include natural materials derived from wastes generated by industry and agriculture, as well as biosorbents that are produced from microbial biomass such as yeasts, fungi, algae etc. (Sulaymon and Abood, 2013; Yang et al., 2012).

Application of fungal biomass to eradicate textile dyes from the effluent is attractive due to its inexpensive and continuous supply from fermentation industry, availability of unsophisticated fermentation techniques for cultivation thereby decreasing the overall effluent treatment costs. Traditionally, the fungal biomass by-product is incinerated for disposal or used as a fertilizer of low economic value for agricultural use. However, it is possible to consider the potential economical reuse of the biomass in the biosorption of dyes (Sag and Aktay, 2002). There are many advantages of using inactivated mycelium for biosorption such as easy storage, selectivity, high removal rates, low costs and regenerative potential. The efficiency of the biosorption process of reactive azo dyes, under equilibrium conditions by some fungi has been shown to be more than that of activated carbon (Ambrosio et al., 2012).

The efficiency of the sorption process is governed by the cost and performance of a sorbent as well as the mode of application. Hence, an attempt was made to evaluate two vital elements of the adsorption process viz. the sorption kinetics and equilibrium of the sorption (Ho and Mckay, 2000; Foo and Hameed, 2010). In this research, four isotherm models viz. Langmuir, Freundlich, Temkin and Dubinin-Radushkevich (D-R) models were used to verify the affinity between *Rhizopus arrihizus* biosorbent and Reactive Orange 13 (RO13), a commonly used monoazo reactive dye in the Indian textile industry. The kinetics data were used to identify the adsorption mechanism and the rate limiting step. Surface characterization of the biosorbent was done using XRD, BET, SEM, FTIR analyses and modification of functional groups on the biosorbent.

EXPERIMENTAL

Materials

Rhizopus arrhizus NCIM 997 used as a biosorbent in this study was obtained from National Chemical Laboratory, Pune, India. RO 13 was obtained as a solid powder from Colourtex Dyes Pvt. Ltd. (Mumbai, India). All the chemicals used in this study were of analytical grade and obtained from HiMedia, India.

Preparation of the biosorbent

Fungal biomass was acquired by aseptically transferring mycelia from the potato dextrose agar (PDA) spread-plate cultures to 100 mL of potato dextrose broth (PDB) (g L^{-1}: potato infusion from 200 g potatoes, dextrose 20, yeast extract 0.1, pH 5.0) containing 0.25 % Tween 80 (to prevent sporulation) in 250 mL Erlenmeyer flasks. The biomass was harvested after seven days of incubation at 30±1^{o}C under static conditions with sporadic shaking. The biomass was then washed thoroughly with double distilled water and dried at 80^{o}C for 24 h. The size of the biomass particles was kept uniform by grinding into a fine powder and sieving through a 150-mesh sieve. Dried biomass was preserved in a desiccator till further use (Saraf and Vaidya, 2015).

Preparation of the adsorbate

Reactive Orange H2R (C.I. Reactive Orange 13, C.I.18270,CAS 12225-85-3, chemical formula: $C_{24}H_{15}ClN_7Na_3O_{10}S_3$, MW: 762.04gmol^{-1}) was used without further purification. Stock solution of the dye (1gL^{-1} at pH 2.0) prepared in double distilled water was diluted to obtain solution of desired concentration (114 mgL^{-1}) for experimental purpose. The pH of the solution was measured using a pH meter (Control Dynamics, India) (Saraf and Vadya, 2015).

ISSN: 2277-9655
Impact Factor: 4.116
CODEN: IJESS7

Characterization of the surface chemistry of the biosorbent

The BET (Brunauer, Emmett and Teller) technique that measures the quantity of gas molecules needed to saturate the solid surface under equilibrium conditions was used to analyze the surface area of the biosorbent before biosorption. A known quantity of the sample (0.0001 g), after drying in an oven at 80ºC for 24 h, was evacuated and then saturated with liquid nitrogen at 77 K using BET Surface Area Dual Component Gas Analyzer SAA-2002. The quantity of the gas required for saturation of the sample was taken as a measure of surface area. The total pore volume (*V*p) was estimated from the volume of N_2 (as liquid) held at a relative pressure. Scanning Electron Microscope (SEM) (Philips XL 30 SEM) was employed to study the surface morphology and fundamental physical properties of the biosorbent surface at 10KV with tilt angle of 45°.The surface structure of biosorbent was analyzed by recording micrographs of suitable magnification with a background subtraction and a summation of 60 scans. X-Ray Diffraction (XRD) analysis, a very powerful tool to study the nature of the biosorbent, was used to assess the presence of crystalline phases present in the biosorbent. X-ray diffraction patterns were recorded in a scanning mode using Rigaku Miniflex X-ray diffractometer equipped with a Cu target having wavelength of 1.54 A˚ with 2θ angle varying between 5º and 80º.Fourier Transform Infrared Spectroscopy(FTIR) (Shimadzu 8400S) analysis of the biosorbent was carried out to identify the characteristic functional groups responsible for biosorption. Each sample was mixed with KBr thoroughly in a proportion of 1:100, using a mortar and pestle, in order to prepare translucent sample discs. These discs were then loaded into the FTIR sample holder and subjected to scan over the IR region (4000 cm^{-1} to 400 cm^{-1}). The infrared spectra were obtained and averaged over 32 scans in the transmission mode. Surface characterization of the dead biomass of *R. arrhizus* using SEM, XRD and FTIR was carried out before and after biosorption with RO 13.

Potentiometric titration of the biosorbent

The potentiometric titration permits quantification of the nature of active (acidic or basic) sites on the sorbent ultimately involved in the dye biosorption.In order to gain a closer insight into the biomass surface properties, a suspension of the biosorbent was potentiometrically titrated applying 0.1N NaOH to reveal the presence of functional groups on the cell wall of the biosorbent. The titration was performed in a 250 mL Erlenmeyer flask using a magnetic stirrer and a pH meter (Control Dynamics, India). Protonation was carried out by soaking 1g of dried biosorbent in 50 mL of 0.1 N HCl and agitating the mixture for 2 h on a rotary shaker at 120 rpm. The titration procedure was executed slowly, by stepwise addition of the titrant (0.1 N NaOH) to the biosorbent slurry. After addition of each 0.25 mL of the titrant, the system was allowed to equilibrate until a stable pH reading was obtained. The potentiometric titration curve was obtained by plotting the volume of the titrant against the recorded pH (Parvathi et al., 2007; Shroff and Vaidya, 2012; Ramrakhiani et al., 2011).

Modification of functional groups on the biosorbent

The chemical modification of amino ($–NH_2$) and carboxylic groups (–COOH) as well as extraction of lipids was carried to study the extent of their involvement in biosorption. Methylation of amines was carried out by treating 1 g of biosorbent with 20 mL of formaldehyde and 40 mL of formic acid. Esterification of carboxylic acids was carried out by suspending 1 g of biosorbent in 65 mL of ethanol and 0.6 mL of concentrated hydrochloric acid. Both the mixtures were shaken separately for 5 h at 150 rpm. Extraction of lipids was carried out by heating 1 g of biosorbent in 75 mL of benzene under reflux conditions for 6 h. After all the treatments, the solutions were filtered using Whatman No. 42 filter paper and the biosorbent was washed with distilled water to remove all the traces of the chemicals and dried at 80ºC for 8 h. The effect of each functional group modification was studied by measuring the change in biosorption capacity of the biosorbent (Parvathi et al., 2007; Shroff and Vaidya, 2012; Ramrakhiani et al., 2011; Kapoor and Viraraghavan, 1997).

Equilibrium studies

Batch biosorption experiments were performed in 250 mL Erlenmeyer flasks containing 50 mL of reaction mixture by using conditions optimized earlier (results not shown) under following conditions: pH 2.0, RO 13 dye concentration 114 mgL^{-1}, biosorbent dosage 0.8 gL^{-1}, temperature 35ºC,speed of agitation 85 rpm. Samples were withdrawn at definite intervals of 20 min over a period of 240 min for determination of the residual colour in the solution after centrifuging at 4000 rm^{-1} for 10 min. The concentration of the dye in the solution was determined from the calibration curve prepared by measuring the absorbance of known concentrations of the dye at 489 nm using UV–Vis Spectrophotometer (Shimadzu, Japan UV1800 UV/VIS)reporting each data point as an average value of the triplicates recorded. Simultaneously a blank without biosorbent was run as a control. The concentration of the dye on the fungal biomass at the corresponding equilibrium conditions were determined using a mass balance equation expressed as specific uptake capacity (SUC) (Akar et al., 2009):

ISSN: 2277-9655
Impact Factor: 4.116
CODEN: IJESS7

$$Q_e = \frac{(C_0 - C_t) * V}{M} \quad (1)$$

Where, C_0 and C_t are the initial and final concentrations of the dye (mgL^{-1}), respectively, M is the biosorbent dosage (g) and V the volume of the solution (L) (Yang et al., 2012; Saraf and Vaidya, 2015).

Isotherm models

In an endeavour to effectively design, develop and optimize an ideal adsorption system and to study the performance of an adsorbent it is essential to establish the most fitting adsorption equilibrium correlation for reliable prediction of the adsorption parameters. In this regard, equilibrium relationships, generally known as adsorption isotherms, describe how pollutants interact with the adsorbents (Foo and Hameed, 2010;Thompson et al., 2001). An adsorption isotherm is critical for predictive modelling and comparing the adsorption performance, optimization of the use of the adsorbent besides providing a view on the degree of affinity of the adsorbent, adsorbent capacities, adsorption mechanism and course taken by the system under study in a concise form. It also indicates economic feasibility of the commercial application of the sorbent under study for a specific solute (Aksu and Tezer, 2005; Itodo and Itodo, 2005; Piccin et al., 2011). In addition, the quality of the fit of experimental results indicates whether adsorption is monolayer or multilayer, on a homogeneous or a heterogeneous surface (Brdar et al., 2012).

The linearized form of Langmuir adsorption isotherm is given below:

$$\frac{C_e}{q_e} = \frac{1}{K_L q_m} + \frac{C_e}{q_m} \quad \textbf{(2)}$$

Where, q_m is the maximum monolayer adsorption capacity (mgg^{-1}), K_L is the Langmuir constant (Lmg^{-1}), and q_e and C_e are the adsorption capacity (mgg^{-1}) and equilibrium concentration (mgL^{-1}), respectively. A straight line of slope $1/q_m$ and intercept $1/K_L q_m$ is obtained by plotting C_e/q_e versus C_e[31].The dimensionless biosorption intensity (R_L) is calculated using the following equation:

$$R_L = \frac{1}{1+(1+K_L C_0)} \quad (3)$$

Where, C_o is the initial concentration of the dye in the solution (mgL^{-1}).

Freundlich isotherm is the earliest known relationship describing the non-ideal, reversible and heterogeneous adsorption due to the diversity of adsorption sites (Freundlich, 1906; Aksu and Donmez, 2003) and its linear expression is given as:

$$\mathbf{\ln(q_e) = ln(K_F) + \frac{1}{n}\ln(C_e)} \quad \textbf{(4)}$$

Where, K_F, an empirical constant, is defined as a sorption coefficient representing the amount of dye molecules for a unit equilibrium concentration and is related to the sorption capacity of the sorbent. Slope, $1/n$ is an empirical constant related to the intensity of sorption and varies with surface heterogeneity and affinity.

Temkin isotherm contains a factor that explicitly takes into account adsorbent- adsorbate interactions. By ignoring the extremely low and high values of concentrations, the model assumes that the adsorption is characterized by a homogenous distribution of binding energies, up to a maximum binding energy (Tempkin and Pyzhev, 1940; Oladoja et al., 2008).The linearized form of Temkin isotherm is given as:

$$\mathbf{q_e = BlnA_T + BlnC_e} \quad \textbf{(5)}$$

Where, B (=RT/b) in (Jmol^{-1}) is related to the heat of adsorption, b is the Temkin's isotherm constant (KJ mol^{-1}) and A_T (Lg^{-1}) = (RTlnAT)/b is the equilibrium binding constant, corresponding to the maximum binding energy. R is the universal gas constant (8.314 Jmol^{-1}K) and T is the absolute temperature (K) (Tempkin and Pyzhev, 1940). A plot of q_e versus ln C_e enables the determination of the isotherm constants B and A_T from the slope and intercept of the straight line plot (Piccin et al., 2011; Oladoja et al., 2008).

Dubinin and Radushkevich developed the following isotherm to account for the effect of the porous structure of an adsorbent (Itodo and Itodo, 2010):

$$\mathbf{Q_e = B_D \exp(-K_D \varepsilon^2)} \quad \textbf{(6)}$$

in which B_D is the Dubinin-Radushkevich isotherm constant related to the degree of sorbate sorption by the sorbent surface representing the theoretical monolayer saturation capacity (mgg^{-1}), K_D (mol^{2}KJ^{-2}) is related to the free

ISSN: 2277-9655
Impact Factor: 4.116
CODEN: IJESS7

energy of sorption per mole of the sorbate as it migrates to the surface of the biomass from infinite distance in the solution and is related to mean adsorption energy (*E*) through

$$E = [\frac{1}{\sqrt{2B_D}}] \quad (7)$$

The Polanyi potential ε is defined by

$$\boldsymbol{\varepsilon = RTln\left[1+\frac{1}{C_e}\right]} \quad \textbf{(8)}$$

It is apparent that the Dubinin–Radushkevich isotherm equation would not be simplified to the Langmuir or Freundlich type of isotherm. Furthermore, plot of lnQ_e versus ln^2(1+(1/C_e) should lead to a straight line, and its slope is given by

$$\boldsymbol{Slope = -B_D R^2 T^2} \quad \textbf{(9)}$$

Thus, the mean adsorption energy (E) can be calculated as follows:

$$\boldsymbol{E = \frac{1}{\sqrt{2B_D}} = \frac{RT}{\sqrt{-2*Slope}}} \quad \textbf{(10)}$$

Where, B_D (mg g^{-1}) is denoted as the isotherm constant representing the theoretical monolayer saturation capacity (Itodo and Itodo, 2010).

Biosorption kinetics

The kinetics represents reaction rates which determine the residence time required for completion of the sorption and elucidates reaction pathways which cannot be explained by the isotherms (Ho, 2004; Crini and Badot, 2008). The kinetics of the reaction was determined with five different kinetic models i.e. the pseudo-first and pseudo second-order rate equations, Elovich, intra-particle diffusion and liquid film diffusion models assuming that the measured concentrations are equal to cell surface concentrations.

One of the most widely used equations for the sorption of the solute from a liquid solution describing the adsorption of liquid-solid systems based on solid capacity is the pseudo-first-order rate equation of Lagergren (Lagergren, 1898). The linear form of Lagergren's pseudo-first-order equation is given as:

$$\log(q_e - q_t) = \log q_e - \frac{k_1}{2.303}t \quad (11)$$

Where, q_e and q_t are the sorption capacity (mg g^{-1}) of the dye at equilibrium and at a time *t*, respectively, and k_1 is the rate constant for pseudo-first order sorption (min^{-1}). A plot of log ($q_e - q_t$) against *t* should give a straight line to confirm the applicability of the kinetic model (Bayramoglu et al., 2006).

The pseudo second-order equation, based on the sorption capacity of the solid phase, predicts the behaviour over the whole range of adsorption and is in agreement with chemisorption mechanism being the rate controlling step and the linear form pseudo-second order kinetic model is:

$$\frac{t}{q_t} = \frac{1}{k_2 q_e^2} + \frac{1}{q_e}t \quad (12)$$

Where, q_e and q_t are the sorption capacity (mgg^{-1}) of the dye at equilibrium and at a time *t*, respectively, and k_2 is the rate constant for pseudo-second order sorption (gmg^{-1}min^{-1}).In the limit $q_t/t = 0$, the initial sorption rate, *h*, is given by $k_2 q_e^2$. Thus, a plot oft/q_t against *t* of equation should give a linear relationship with a slope of $1/q_e$ and an intercept of $1/k_2 q_e^2$, i.e. 1/*h* (Ho et al., 2002).

Elovich equation is used successfully to describe second order kinetics assuming that the actual solid surfaces are energetically heterogeneous, but the equation does not propose any definite mechanism for adsorbate–adsorbent (Ho and Mckay, 1998). The linear form of the Elovich model is presented by the following equation:

$$q_t = \frac{1}{\beta}\ln(\alpha\beta) + \frac{1}{\beta}\ln(t) \quad (13)$$

The constants α and β were obtained from the slope and intercept of the linear plot of q_t versus ln*t* (Bulut et al., 2008).Teng and Hsieh (1999) proposed that constant α is related to the rate of chemisorption while β is related to the surface coverage. A higher value of α indicates an efficient adsorption mechanism (Aroua et al., 2008).

ISSN: 2277-9655
Impact Factor: 4.116
CODEN: IJESS7

The prediction of the rate-limiting step is important in the adsorption processes. It influences design and scale-up of the process. The mechanism of adsorption is generally considered to involve one or any combination of the rate-controlling mechanisms: bulk diffusion, film diffusion, pore diffusion or intra-particle diffusion and chemical adsorption of dye at an active site on the surface. Bulk diffusion is non-limiting when agitation is sufficient to avoid concentration gradients in solution. So, the most important steps are film diffusion, pore diffusion and chemical reaction. Therefore, adsorption diffusion models were constructed to describe the process of film diffusion and/or intra-particle diffusion because the pseudo-first-order and pseudo-second-order models cannot identify the diffusion mechanism (Weber and Morris, 1963; Qui et al., 2009). Weber and Morris (1963) described the intra-particle uptake of the adsorption process to be proportional to the half-power of time. The intra-particle diffusion rate constant (k_{id}) is given by the following equation:

$$q_t = k_{id} * \sqrt{t} \quad (14)$$

This parameter, although not a reaction rate, can be correlated with system variables to characterise the influence of intra- particle diffusion.

When the boundary plays the most significant role in adsorption during the transport of the solute molecules from the liquid phase up to the solid phase; the liquid film diffusion model may be applied as follows:

$$\ln(1 - F) = -k_{fd}t \quad (15)$$

Where, F is the fractional attainment of equilibrium $F = q_t/q_e$ and k_{fd} is the external mass transfer coefficient ($Lmin^{-1}$). A zero intercept would suggest that the kinetics of the adsorption process is controlled by diffusion through the liquid film surrounding the solid adsorbent (Oladoja et al., 2008; Aroua et al., 2008; Boyd et al., 1947).

Error Analysis

Determination of the best isotherm or kinetics model though possible through analysis of the correlation coefficient (R^2), is not sufficient and can lead to some ambiguities when the set of data is not complete. The linearization of isotherm equations using data transformations will implicitly alter the error structure and may also violate the error variance and normality assumptions of standard least squares. Due to the inherent bias from linearization, alternative isotherm parameter sets were determined by non-linear regression. This provides a mathematically meticulous method for determining the isotherm parameters by using the original form of the isotherm equation (Brdar et al., 2012). In all of the error analysis methods it is assumed that both the liquid-phase concentration and the solid-phase concentration contribute equally to weighting the error criterion for the model solution procedure (Allen et al., 1989). The suitability, applicability and fitness of different isotherm and kinetics models to the biosorption were assessed on the basis of the closeness of the estimated maximum biosorption capacity to the experimental biosorption maximum using five error analysis methods. The lower the numerical value of these error functions for a given equation, the better is the fit for that equation (Piccin et al., 2011; Allen et al., 1989):

The Sum of Squared Errors (SSE) (Eq.16) is the most commonly utilized error function. It is assumed that the model which gives the lower SSE values is the best model for dye sorption.

$$SSE = \sum_{i=1}^{n} \left(q_{e,calc} - q_{e,meas}\right)^2 \quad (16)$$

In Sum of absolute errors (SAE)(Eq. 17), the approach is similar to the SSE method. Isotherm parameters determined using this error function provides a better fit as the magnitude of the error increases, biasing the fit towards the high concentration data.

$$\text{SAE} = \sum_{i=1}^{n} \left| q_{e,calc} - q_{e,meas} \right|_i \quad (17)$$

The average relative error (ARE) (Eq.18) function attempts to minimize the fractional error distribution across the entire concentration range.

$$ARE = \frac{100}{n} \sum_{i=1}^{n} \left| \frac{q_{e,calc} - q_{e,meas}}{q_{e,meas}} \right| \quad (18)$$

Hybrid fractional error function (HYBRID) (Eq. 19), a composite fractional error function was developed in order to improve the fit of the SAE method at low concentration values (Brdar et al., 2012).In this method each SAE value is divided by the experimental solid-phase concentration value q. In addition a divisor is included as a term

ISSN: 2277-9655
Impact Factor: 4.116
CODEN: IJESS7

for the number of degrees of freedom for the system—the number of data points minus the number of parameters within the isotherm equation.

$$HYBRID = \sum_{i=1}^{n}\left[\frac{(q_{e,meas}-q_{e,cal})^2}{q_{e,meas}}\right]_i \quad (19)$$

The Marquardt's percent standard deviation (MPSD) (Eq. 20) is similar in some respects to a geometric mean error distribution modified according to the number of degrees of freedom of the system.

$$MPSD = \sum_{i=1}^{n}\left[\frac{q_{e,meas}-q_{e,cal}}{q_{e,meas}}\right]_i^2 \quad (20)$$

Where $q_{e,\ calc}$ are the theoretical adsorbed solid phase concentrations of sorbate on sorbent, which have been calculated from one of the isotherm equations and $q_{e,meas}$ are the experimentally determined adsorbed sorbate concentrations obtained from Eq. (1) using the experimentally measured equilibrium sorbate liquid phase concentrations, C_e (Saraf and Vaidya, 2015).

Desorption and reuse of the biosorbent

The dye loaded biosorbent prepared by exposing the dried biomass of *R. arrhizus* (0.8 g L^{-1}) to RO 13 solution (114 mg L^{-1}) at pH 2.0 for 120 min at 35ºC on a rotary shaker (85 r m^{-1}) was used for desorption. The biomass sorbed with RO13 was separated by centrifugation at 4000rm^{-1} for 10 min, washed repeatedly with deionized water to remove any residual dye and dried at 80°C for 24 h before use. The amount of RO 13 absorbed after 120 min of contact time was calculated to be 133.63mgg^{-1}[20].Desorption studies were initially optimized using this pre-loaded biosorbent of *R. arrhizus* by using solutions of different molarity (0.001, 0.0015, 0.0025, 0.005, 0.01, 0.1) of NaOH as eluants at a constant solid to liquid ratio (S/L) of 10, in 250 mL Erlenmeyer flasks. The desorption of the dye was optimized over a range of S/L of 2, 5, 8, 10, 15, 20, 25, 30, 40 and 50 using the molarity of NaOH that yielded the highest desorption (Shroff and Vaidya, 2011; Tunali et al., 2005). Each desorption cycle was allowed 200min of contact time. The eluted biosorbent was washed repeatedly with deionized water to remove any residual desorbing solution and placed into dye solution for the succeeding biosorption cycle after drying to a constant weight. The cycles were repeated five times using the same biomass (Shroff and Vaidya, 2011).

Desorption efficiency was calculated by using following equation:

$$Desorption\ efficiency = \frac{Amount\ of\ dye\ desorbed}{Amount\ of\ dye\ adsorbed} * 100 \quad (21)$$

RESULTS AND DISCUSSION

Characterisation of biosorbent

BET analysis

The surface area, pore diameter and the pore volume of the biosorbent were found to be 0.618m^{2}g^{-1}, 6.4789nm and 0.001ccg^{-1}respectively.Dubinin (1967) suggested that the pore structure of adsorbent particle consists of macropores, intermediate or transitional mesopores and micropores. Large molecules like dyes can diffuse inside the mesopores more effectively than diffusion through the micropores of the adsorbent. In a similar study, Nakagawa et al.(2004) have shown that mesoporous activated carbons were more effective in removing large sized reactive dye molecules compared to microporous activated carbons. High biosorption values achieved (Saraf and Vaidya, 2015) despite low surface area (0.618m^{2}g^{-1}) could thus be attributed to the mesoporous structure of the biosorbent.

SEM Analysis

Scanning electron microscopy (SEM) has been a primary tool for characterizing the surface morphology and fundamental physical properties of the adsorbent surface. It is useful for determining the particle shape, porosity and appropriate size distribution of the adsorbent (Namasivayam and Kavitha, 2002).The morphological profile of the biosorbent revealed a rough and heterogeneous surface with relatively porous matrix of macroporous character, pointing towards its potential in taking up the dye. Fig. 1b shows the change in the structure of the biosorbent after sorption with RO 13 showing less porous structure indicating effective adsorption of dye molecules in the pores, interstices and cavities on the external surface of this biosorbent. The macropores facilitated easy diffusion of RO 13 into the pores and also assisted adsorption of dye molecules on the surface of the biosorbent.

ISSN: 2277-9655
Impact Factor: 4.116
CODEN: IJESS7

Fig.1- Scanning electron micrographs of a) Biosorbent before biosorption and b) Biosorbent after biosorption of RO 13

XRD analysis

The XRD pattern of *R. arrhizus* revealed poorly resolved peaks indicating a predominance of amorphous nature thereby proving the suitability of the biosorbent for biosorption. The XRD spectra of *R. arrhizus* biosorbent revealed broad peaks at 2θ of 19.7572, 21.4273, 24.0244 and a small sharp peak at 2θ of 72.6714 with *d* spacing 4.49365, 4.14703, 3.70429 and 1.30113.Presence of broad peaks can be attributed to a heterogeneous and complex matrix composed of several substances, including proteins, lipids, carbohydrates etc. Adsorption of dye may lead to change in molecular and crystalline structure of the adsorbent as was evident from the XRD pattern of the RO 13 laden biosorbent. The XRD pattern of the dye loaded biosorbent showed two crystalline peaks at 2θ of 43.5844 and 49.1604 which is suggestive of adsorption of crystalline dye molecules mostly by chemisorption causing alteration in the structure of the biosorbent (Namasivayam and Kavitha, 2002).

Fig. 2 - XRD pattern of a) Biosorbent after biosorption of RO 13 and b) Biosorbent before biosorption

Potentiometric titration

The qualitative and semi-quantitative determination of the nature of active (acidic or basic) sites present on the cell wall of the biosorbent was carried out by potentiometric titration as shown in Fig. 3.The diversity of the functional groups in biomaterials of the organic constituents has proposed that the acid-base potentiometric titration method, can help to (1) estimate the cationic exchange capacities of different kind of organic materials, (2) identify the acid ionizable functional groups (binding sites) which can play the role of ligand in the presence of protons and (3) describe the chemical heterogenic reactivity of the organic surface (Naja et al., 2005).

The potentiometric titration data indicated that the fungal surface exhibited a significant buffering capacity over the entire pH range studied and showed presence of various functional groups. The curve in Fig. 3 showed five inflexion points at approximately pH 3.43, 4.18, 5.46, 9.52 and 10.84. It may be inferred that acidic groups were carboxylic groups (pK_a2.5-5.2). The pK_a of 2.5 corresponds to a carboxylic moiety linked to an aromatic group, while the pK_a of 5.2 is attributed to a carboxylic moiety linked to an aliphatic chain. The pK_a value obtained in the present work (5.46) indicated that the carboxylic acidic groups in the *R. arrhizus* biomass examined were linked to aliphatic chains rather than to aromatic groups. The proximity of another carboxylic group could be responsible for a higher ionization and lower pK_a values (Naja et al., 2005). Parvathi et al. (2007) reported a similar inflexion point for a carboxyl group at 5.60. The alkaline groups were comparable to the values reported for the amine ionization constants (pK_a) of the proteins or polypeptides (pK_a8.1-11.0), sulfhydryl (thiol) (pK_a 8.0–10.0) and hydroxyl (pK_a 9.5–13.0), the saturated amines (pK_a8.5 -12.5) or phenolic acidic groups with ionization constants between 9.9 and 10.8 depending on the different substitutions of the phenolic groups (Parvathi et al., 2007; Ramrakhiani et al., 2011; Naja et al., 2005; Volesky, 2007).

Fig.3-Potentiometric titration curve

FTIR analysis

The biosorptive removal of the dyes by the fungal biosorbent is mainly linked to the composition of the cell wall, which is considered as the primary site of bio-availability. The hexosamines-chitin and chitosan constituting approximately 24–40% of the cell dry weight of *Rhizopus* along with proteins and lipids serve as a matrix of various functional groups like amine R–NH_2 (amino acids, proteins, glycoproteins, etc.), carboxylic (fatty acids, lipopolysaccharides, etc.), which take part in binding of dye ions (Tsezos, 1983). A closer insight into the biomass surface properties was obtained by comparing the FTIR spectra of biomass of *R. arrhizus*, before and after biosorption with RO 13 in the range of 400–4000 cm^{-1}(Fig. 4).The infrared spectrum of the biosorbent displayed the complex and heterogeneous nature showing characteristic bands of proteins, lipids and polymeric compounds. Despite the complexity, certain typical characteristic peaks could be assigned to functional groups (Arica and Bayramoglu, 2005).

Peaks between 3500 to 3200 cm^{-1} represent–OH groups of alcohols and phenols and primary, secondary amines or amide –N-H groups, while peaks between 3300 to 2500 cm^{-1} indicate O-H stretch of carboxylic acids (Chen et al., 214). Peak positions between the wave number range of 2000 cm^{-1} to 500 cm^{-1}, indicate the vibrational modes that are specific to the type of polysaccharides and glycosidic linkages and denote the presence of aldehyde groups which are actively involved in biosorption. Amide I bands (1700-1600cm^{-1}) due to C=O stretching vibrations of peptide bonds provide insight into the protein secondary structure (Abirami et al., 2013). Peaks between 910-665 cm^{-1} represent N-H wag of primary and secondary amines.

ISSN: 2277-9655
Impact Factor: 4.116
CODEN: IJESS7

The FTIR spectra of the biosorbent exhibited appearance, disappearance and shifting of various peaks with change in intensity due to change in bonding energy in the corresponding functional groups after biosorption. This confirmed changes in the availability of the functional groups and active role played by them in biosorption. Peaks at 3523.95-3302.13 cm^{-1} indicate the presence of carboxyl, primary and secondary amines as well as amides. Disappearance of peaks at 3302.13$cm^{-1}$and shifting of peak from 3523.95 to 3514.3cm^{-1}indicates their involvement. The spectrum displayed the absorption peaks at 1743.65, 1710.86, and 1238.3 cm^{-1}, corresponding to carboxyl groups. Shifts in peaks corresponding to carboxylic groups (1238.3 to 1224.8 cm^{-1}) and disappearance of peaks at 1743.65, 1710.86 cm^{-1} indicates their participation. Disappearance of peaks at 3226.91 $cm^{-1}$and shifting of peak at 1539.2 to 1537.27cm^{-1} indicated the contribution of amine groups in the binding of RO 13. Shifting of bands from 3282.84 to 3280.92cm^{-1}; 2852.72 to 2854.65 cm^{-1}, 1159.22 to 1161.15 $cm^{-1,}$ and 1031.92 to 1035.77 cm^{-1} indicated the involvement by C-O stretching vibrations, NH bending, C-O-C linkage, bonded hydroxyl OH of water in binding of the dye when compared to that of the biomass of *R. arrhizus* before biosorption (Florence et al., 2015). Several bands in the range of 1658.78-1379.10 $cm^{-1}$are assigned to phenolic and amine groups [67]. The disappearance of peak at 1379.10 cm^{-1}after binding of RO 13 indicated their participation in the biosorption (Smith, 1999; Cardoso et al., 2010).The peaks at 2924.09 cm^{-1} can be attributed to asymmetric C—H stretching vibrations of methyl, methylene and methoxy groups did not change even after biosorption with RO 13, indicating that these groups did not participate in the biosorption process. FTIR technique proved to be an efficient tool for detecting the structural changes and probable binding sites induced by the biosorption of RO 13.

Fig.4 - FTIR spectra of a) Biosorbent before biosorption and b) Biosorbent after biosorption of RO 13

Modification of the functional groups

The potential functional groups implicated in biosorption by FTIR analysis, were blocked by chemical treatments to study the extent of their involvement by measuringthe percent reduction in the biosorption. The treatment of the biosorbent with formic acid (HCHO-HCOOH) causes blocking of primary and secondary amines on the biosorbent due to their methylation (Parvathi et al, 2007). The reaction occurs as follows:

$$RCH_2NH_2 \xrightarrow{HCHO+HCOOH} {}_2N(CH_3)_2 + CO_2 + H_2O$$

The methylation of the amino groups strongly affected the removal of RO 13 by *R.arrhizus* showing a significant reduction of 48.26 % in biosorption. This reduction can be attributed to prevention of their participation in dye biosorption, indicating a major role played by amino groups in biosorption of RO13.Chitin carries one linear amino group per glucose unit and thus exhibits a high dye uptake capacity (Naja et al., 2005; Tsezos, 1983).

Treatment of the biosorbent with ethanol results in esterification of carboxylic acids causing reduction in the number of positively charged sites present on the cell wall of the biosorbent and the reaction occurs as follows [21]:

$$RCOOH + CH_3OH \xrightarrow{H^+} RCOOCH_3 + H_2O$$

Esterification of the carboxyl groups decreased the biosorption of RO 13 by 5.76% indicating that carboxylic groups also to some extent contributed to biosorption of RO 13. However, the role of carboxylic acids seemed to be minor to that of amines. Since RO 13 has only one NH_2 group in the dye molecule, interactions between carboxyl and carbonyl groups of the biosorbent and NH_2 group of the dyes maybe less important than that of NH_2 groups of biosorbent and SO_2^{-3} groups of the dye (Yang et al., 2012).

Removal of lipids from the biosorbent also exhibited a negative effect causing a slight reduction of 1.11% in the biosorption of RO 13, which revealed the contribution of lipids present on the cell wall of *R. arrhizus* in biosorption. The decrease in biosorption can be attributed to possible structural changes that may have occurred due to the harsh conditions employed for the extraction process (Ramrakhiani et al., 2011).

Isotherm studies

The shape of an isotherm can predict if a sorption system is favourable or unfavourable. The isotherm shape can also provide qualitative information on the nature of the solute–surface interaction (Crini and Badot, 2008). The shape of the isotherm for RO 13 biosorption by *R. arrhizus* showed L2- type behaviour (i.e. a concave shape and a plateau) according to the Giles and Smith classification (Giles et al., 1974). In L2-type isotherms, adsorption of solute on the adsorbent proceeds until a monolayer is established, the formation of more than one layer being

ISSN: 2277-9655
Impact Factor: 4.116
CODEN: IJESS7

impossible. Based on the type of the isotherm, four widely used mono-component isotherm models were employed to study the biosorption of RO 13 on the *R. arrhizus* biosorbent(Table 1).

Table 1- Isotherm parameters and error analysis for adsorption of RO 13 on *R. arrhizus*

The essential characteristics of the Langmuir isotherm, expressed in terms of a dimensionless constant separation factor or equilibrium parameter, R_L, indicates the nature of adsorption to be either unfavorable (R_L> 1), linear (R_L = 1), favorable (0 <R_L< 1) or irreversible (R_L = 0) (Ilhan et al., 2008). The low R_L value(0.007)obtained in the present investigation indicated that the adsorption of RO 13 onto the biosorbent is favorable. A high value of Langmuir parameter q_{calc}(137.09 mg g^{-1}) is suggestive of high biosorption capacity of the biosorbent and predicts monolayer sorption. The second Langmuir parameter K_L reflects the affinity of a sorbent for a particular dye ion. Langmuir isotherm model fitted the results reasonably well (R^2= 0.999), suggesting that the surface of the sorbent could be homogenous and attainment of saturation during dye biosorption was achieved. It also indicated that the sorbed molecules are organized as a reversible monolayer, all the sites are energetically equivalent and there is no interaction between the sorbed molecules. However, biosorption sites on the fungi are not homogeneous, as presumed in the Langmuir model, because they contain functional groups of diverse kind, which vary in their affinity for dye ions.

The Freundlich isotherm model for sorption of RO 13 also fitted well yielding a straight line. The values of 1/*n* and K_F were calculated from the slope and intercept of the plot of ln q_e versus lnC_e. The K_F is found to be primarily related to the capacity of the adsorbent for the given ion; the higher the value of K_F the larger is the capacity of sorption. A very high value of K_F (160.77) indicated a high sorption capacity of the biosorbent for RO 13. Freundlich isotherm constant 1/*n* can be used to calculate the adsorption capacity and intensity of the reaction and to explore the favourability of adsorption process. The slope 1/*n* value indicates the type of isotherm to be irreversible (1/*n* = 0), favorable (0 < 1/*n* < 1), unfavorable (1/*n*>1). A value of 1/*n* = 1 shows that the partition between two phases does not depend on the concentration, while 1/*n*> 1 indicates a cooperative sorption involving strong interactions between the molecules of adsorbate. Isotherms with value of 1/*n* below unity are classified as L-type isotherms reflecting a high affinity between adsorbate and adsorbent and are indicative of chemisorption. In the present investigation values of 1/*n* below one (0.096) indicated chemisorption (Foo and Hameed, 2010; Ilhan et al., 2008). Conformity to the Freundlich model indicated that the biomass was completely saturated and the dye ions were adsorbed reversibly onto the surface in a multilayered pattern. The regression coefficient (R^2) value 0.97 for RO 13was lower compared to Langmuir model, which can be attributed to assumption of the Freundlich model that dye biosorption does not saturate. However, isotherm curve of RO 13 clearly depicted saturation of dye ions. Thus, the Freundlich model is less appropriate than Langmuir model for defining dye biosorption by the biosorbent, even though its parameters do convey some important information regarding dye biosorption and intensity Dhananjay et al., 2010).

The linear plot for Temkin adsorption isotherm, which considers monolayer chemisorption of an adsorbate onto the adsorbent, fitted quite well (R^2=0.975). This further supports the findings that the adsorption of RO 13 onto the biosorbent occurs by a chemisorption process (Fiorentin et al., 2010). The D–R isotherm equation has been often used to determine the mean adsorption energy (*E*) that may provide useful information with regard to whether or not biosorption is subject to a chemical or physical process (Liu and Liu, 2008). The D-R isotherm model is more general than the Langmuir isotherm as its deviations are not based on ideal assumptions such as equipotential of sorption sites, absence of steric hindrances between sorbed and incoming particles and surface homogeneity on microscopic level. In the present study, the estimated constant, B_D, related to adsorption energy was $5*10^{-7}$ mg g^{-1}. This constant gives an idea about the mean free energy which was valued as *E*= 1.0 KJ mol^{-1}. *E* is a parameter used in predicting the type of adsorption. Based on this energy of activation one can predict whether an adsorption is physisorption or chemisorption (Itodo and Itodo, 2010). However, deviation from the measured SUC of the biosorbent for RO 13and low value of R^2 (0.823) showed that D- R isotherm model did not give very good description of the sorption process. Thus, it can be assumed that the sorption takes place by chemisorption as suggested by Langmuir, Freundlich and Temkin isotherms though the data were described well by the Langmuir model based on error analysis (Table 1)

Kinetic studies

An ideal adsorbent for wastewater pollution control must not only have a large adsorbate capacity but also a fast adsorption rate. The kinetics data supply the solute uptake rate, which determines the residence time required for

ISSN: 2277-9655
Impact Factor: 4.116
CODEN: IJESS7

completion of the sorption reaction and give the complete description of the transport mechanisms of adsorbate on the adsorbent (Ho, 2004; Crini and Badot, 2008).

Table 2- Kinetic parameters and error analysis for adsorption of RO 13 on *R. arrhizus*

It has been reported that the Lagergren's model does not fit the kinetic data well for the entire range of contact time and is generally valid over the initial 20–30 min of the sorption process, and results generally show highly varied q_e values as seen in this study (Ho and Mckay, 2000; Binupriya et al., 2010). The reason for this difference in the q_e value is that there is a time lag at the beginning of the sorption process, possibly due to a boundary layer or external resistance control (Mckay et al., 1999). Thus, the adsorption of RO13 on the biosorbent did not follow the pseudo-first order adsorption kinetics. On the other hand, a correlation coefficient (R^2) of 0.999 and the proximity of the experimental equilibrium capacity $q_{e,\,exp}$ estimated from the pseudo-second order kinetics with theoretical $q_{e,\,cal}$ value indicated a good compliance with the pseudo second-order equation. This suggests that the sorption system fits the pseudo- second order model, based on the assumption that the rate limiting step may be chemisorption (Aksu and Tezer, 2005; Qui et al., 2009). The biosorption data were further analyzed using the Elovich equation. It has extensively been accepted that the chemisorption process can be described by this semi-empirical equation (Aksakal and Ucun, 2010). Teng and Hsieh (1999) proposed that constant α is related to the rate of chemisorption while β is related to the surface coverage. The constants depend significantly on the amount of adsorbent with the adsorption constant, α, being a more sensitive parameter. A good biosorption process is indicated by a higher value of α, as seen in this case. The correlation coefficient of Elovich equation (0.93), was lower than that of the pseudo second-order equation. The Elovich equation does not predict any definite mechanism, but it is useful in describing adsorption on highly heterogeneous adsorbents. This situation indicates that the Elovich equation may also be used to predict the adsorption kinetics of RO 13 onto the biosorbent for the entire adsorption period since the biosorbent possesses heterogeneous surface active sites such as amines, carboxyl, hydroxyl groups etc.

The relatively short contact time, necessary for achieving equilibrium conditions (three hours as seen in this study), apart from the evident processing advantages, is considered as an initial indication that adsorption of dyes on *R. arrhizus* is chemical-reaction controlled, rather than a diffusion controlled process (Ho and Mckay, 2000). A more appropriate quantitative approach to distinguish between kinetic and diffusion rate control is to perform the square root of contact time analysis. The plot of q_t versus $t^{0.5}$ for RO13, presents multi-linearity implying that more than one process affected the adsorption, which was also shown in previous studies (Fig. 5) (Crini and Badot, 2008; Juang et al., 1997). The first, sharper portion was attributed to an instantaneous adsorption stage of diffusion of dyes through the solution to the external surface of the biosorbent, or the boundary layer diffusion effect (i.e., external film resistance) of solute molecules. The second portion described the gradual adsorption stage of intra-particle diffusion (macro- and mesopore diffusion). The third portion was attributed to the final equilibrium stage where the dye is adsorbed on sites on the interior surface of the biosorbent. This stage is assumed to occur very rapidly and does not form a rate-limiting stage in the adsorption of dyes onto the biosorbent. The intra-particle diffusion also starts to slow down due to the extremely low dye concentration left in the solution. The rate of uptake might be limited by the size of adsorbate molecule, concentration of the adsorbate and its affinity to the adsorbent, the pore-size distribution of the adsorbent (Guibal et al., 1998).

Fig. 5 -Intra-particle diffusion model

The rate constant k_{id} (mg g^{-1} $min^{-1/2}$) of the intra-particular diffusion on the biosorbent was low probably indicating slow diffusion of the bulky molecule of RO 13 during the adsorption process. According to Weber and Morris (1963), if intra-particle diffusion is involved in the adsorption process, then the plot of the square root of time versus the uptake would result in a linear relationship and intra-particle diffusion would be the rate-limiting step if this line passed through the origin. The deviation of the straight line from the origin is indicative of some degree of boundary layer control and further shows that the intra-particle diffusion is not the only rate controlling step, but that other processes may control the rate of adsorption (Aksakal and Ucun, 2010).The extrapolation of the linear straight line to the time axis gives intercept *C*, which is proportional to the boundary layer thickness. This is attributed to the instantaneous utilization of the most easily available adsorbing sites on the adsorbent surface (Crini and Badot, 2008;Kaur et al., 2013). In the present study, a very large value of *C* suggests a greater boundary layer effect and greater contribution of the surface adsorption in the rate limiting step (Vasanth kumar and Porkodi, 2007).

The linear plot of –ln (1-*F*) vs. *t* whereby $F = q_t/q_e$, despite providing good linearity does not pass through the origin (Fig.6). Thus, it can be concluded that liquid film diffusion is not the predominant mechanism for RO 13

ISSN: 2277-9655
Impact Factor: 4.116
CODEN: IJESS7

adsorption on the biosorbent. Error analysis revealed that the second order kinetic model best described the biosorption of RO 13 on the biosorbent.

Fig. 6- Liquid film diffusion model

Desorption and reuse of biosorbent

One of the key factors in assessing the potential of the biosorbent for commercial application is its regeneration (Tunali et al., 2005). Desorption studies not only help to elucidate the nature of adsorption, they are also critical in keeping the costs down while recovering the dye non-destructively from the liquid phase in a concentrated form, facilitating its disposal and thus restoring the biosorbent for effective reuse. The potential reusability and the stability of the biosorbent were assessed by monitoring the change in recovery through five consecutive adsorption– desorption cycles of 200 min each.

As the molarity of NaOH increased (S/L at 10) from 0.001 M to 0.01 M, the percent desorption increased from 3.4 to 99.73 %. This can be attributed to the increase in negative OH^- ions creating a negatively charged surface on the biosorbent which favoured desorption of dye anions due to the electrostatic repulsion (Arami et al., 2008). Use of 1 M NaOH reduced desorption similar to the trend reported by Arami et al. (2005), Kadirvelu et al. (2005), Patel and Sumathi (2008) during desorption of dyes from orange peel, activated carbon and *Aspergillus foetidus*, respectively. The efficiency of the desorbing agent is often expressed by the solid to liquid ratio (S/L). High values of S/L are desirable for complete elution and to make the process more economical (Gupta et al., 2000). However, at the same time, the volume of the solution should be enough to provide maximum solubility for the dye desorbed. Hence, using 0.1 M NaOH as an eluant, S/L was optimized from 2 to 50.The desorption increased with increase in S/L from 2 to 10 yielding highest value (99.73%) at S/L of 10, decreasing thereafter (Fig. 7). The biosorbent undergoing successive adsorption–desorption cycles retained good adsorption capacity even after five cycles and only a maximum of 4.14 % decrease in sorption capacity was observed after five cycles. The diminished effectiveness of adsorption and desorption in the subsequent cycles may result from the depletion of active sites of the sorbent being occupied by the dye (Filipkowska et al., 2004). This confirms that the adsorption process was chemical adsorption.

Fig. 7-Sorption desorption cycles for RO 13 dye

Mechanism of Sorption

For design purposes determining the adsorption mechanism is important. The adsorption mechanism often depends on the sorbent characteristics (surface area, particle size, surface polarity and pore size distribution other than surface functional groups) or to sorbate structural features (molecular weight, shape, molar volume, flexibility, branching, etc.). When pore diffusion is the rate-limiting step, the internal pore diameter of the biosorbent as compared to the molecular size of the adsorbate and the adsorption capacity of the adsorbent are key design factors. Porosity of the sorbent controls the diffusion to the center of the particles (Crini and Badot, 2008). The possibility of intraparticle diffusion of dye ions from the surface into the pores of sorbent was elucidated by the BET analysis. BET analysis revealed abundance of mesopores which are instrumental in the transport of adsorbate molecules to the micropores. According to Dubinin (1967), the pore size distribution is of more importance than the surface area. When pores are large enough to admit one dye molecule but too small to admit another one, the pore blockage may be the dominant competition mechanism, which is not the case for the biosorbent used in this study. This was further highlighted by the calculation of molecular dimensions of RO13 (assuming a planar geometry of molecules) and optimized three-dimensional structural formula using ACD/LABS version 10.0. The longitudinal and axial length of RO 13 is 2.1212 nm and 1.2009 nm, respectively (Fig. 8). The average pore diameter of the *R. arrhizus* biosorbent is 6.4789 nm, indicating easy diffusion of RO 13 within the mesopores. Assuming that the entrance of the mesopores is circular in shape, the area of the entrance is 32.95nm^2. The estimated molecular area of RO 13 is 2.55nm^2, which endorses easy access of the dye into the mesopores ruling out pore diffusion as the rate limiting step.

Fig. 8- Molecular dimensions of RO13 using ACD/LABS version 10.0

The fitting of the experimental data to both Langmuir and Freundlich isotherm models suggested that the biosorption process was a monolayer capacitive sorption process in which homogeneous and heterogeneous biosorption patches coexisted on the surface of *R. arrhizus* and the biosorption process involved more than one mechanism. The goodness of fit provided by pseudo second-order equation suggested that the rate limiting step

ISSN: 2277-9655
Impact Factor: 4.116
CODEN: IJESS7

may be chemisorption. A greater boundary layer effect shown by intra-particle diffusion model suggested a greater contribution of the surface adsorption in the rate limiting step. Similar results were reported by Uzun (2006).

Generally, electrostatic attraction between the negatively charged dye anions and the positively charged cell surface is commonly cited as the main sorption mechanism (Crini and Badot, 2008; Juang et al., 1997). FTIR analysis and modification of amino groups also indicated a dominant sorption mechanism involving electrostatic interaction between anionic groups i.e. three SO_3^{-2} groups of RO 13 and protonated amine/imine groups of the biosorbent (Aksu and Tezer, 2005; Crini and Badot, 2008). Simultaneously, interactions between the sorbent matrix and numerous benzene rings in the dye molecule, as well as hydrogen bonding, could play an important role. The availability of amine groups is controlled by two important parameters: the crystallinity of the polymer and the diffusion properties (Crini and Badot, 2008). Predominance of amorphous nature revealed by the XRD analysis indicated the accessibility of adsorption sites and thus the suitability of the biososrbent for biosorption. In order to confirm the electrostatic attraction of the positively charged biosorbent surface at pH 2.0 with the negatively charged dye, desorption experiments were carried out. If the adsorbed dye on the solid surface can be desorbed by water, then the attachment is by weak bond or physisorption. Since no desorption of Reactive Orange 13 occurred in water, it seems that most of the dye is adsorbed through chemisorptions (Namasivayam and Kavitha, 2002).

Overall, the sorption process can be described as follows: RO 13 is first adsorbed on the surface of *R. arrhizus* by chemisorption via electrostatic interaction until the surface functional sites are fully occupied; thereafter dye molecules diffuse into the pores of the biosorbent layers for further interactions (Crini and Badot, 2008;Bulut et al., 2008; Altaher et al., 2014).

CONCLUSION

R. arrhizus, a low cost waste biomass from industrial fermentations proved to be a promising biosorbent due to a short equilibrium time and high specific uptake capacity. The XRD pattern of *R. arrhizus* revealed preponderance of amorphous nature thereby proving the suitability of the biosorbent for biosorption. The heterogeneous surface with relatively porous profile of the biosorbent was revealed by SEM analysis. Langmuir, Freundlich and Temkin isotherm models fitted the adsorption equilibrium data with high correlation coefficients, though the Langmuir model described the data most efficiently. The suitability of the pseudo-second order equation for the sorption of RO 13 pointed towards chemisorption as the mechanism of biosorption. The experimental data also showed that intra-particle diffusion is significant in determination of the sorption rate. FTIR analysis and modification of functional groups indicated contribution of amino and carboxyl groups in biosorption. Desorption and reusability studies using RO 13 loaded biomass, showed potential for the recovery and the further containment of RO 13. Use of 0.1 M NaOH as eluantat S/L of 10 proved to be beneficial. The biosorbent could be regenerated and reused at least five times in biosorption–desorption cycles successively.

Figures and tables

Fig.1- Scanning electron micrographs of a) Biosorbent before biosorption and b) Biosorbent after biosorption of RO 13

a) b)

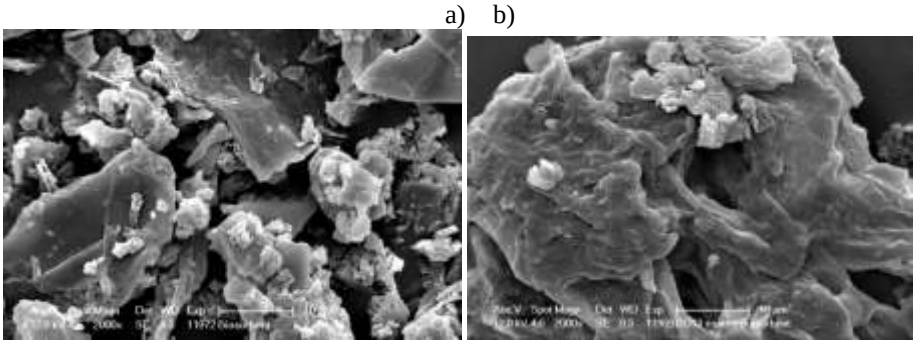

Fig. 2 - XRD pattern of a) Biosorbent after biosorption of RO 13 and b) Biosorbent before biosorption

ISSN: 2277-9655
Impact Factor: 4.116
CODEN: IJESS7

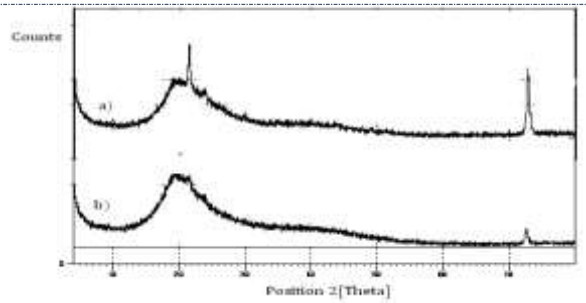

Fig.3-Potentiometric titration curve

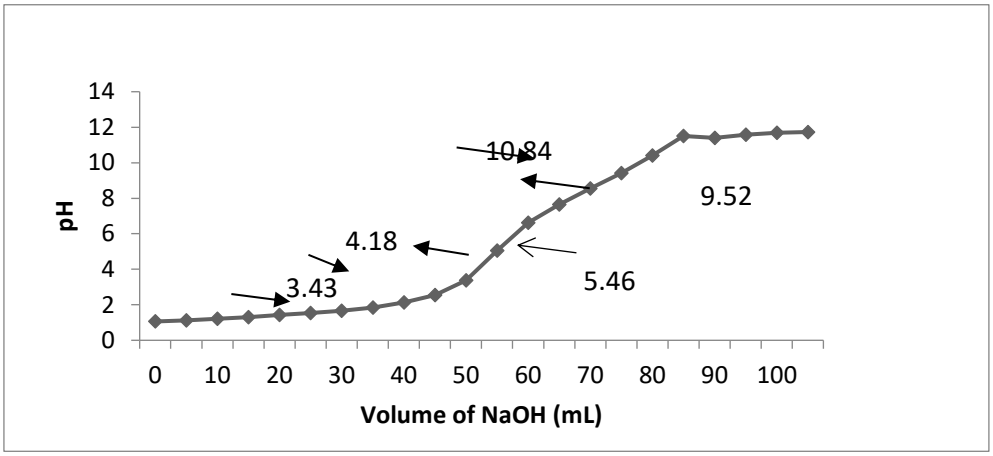

Fig.4 - FTIR spectra of a) Biosorbent before biosorption and b) Biosorbent after biosorption of RO 13

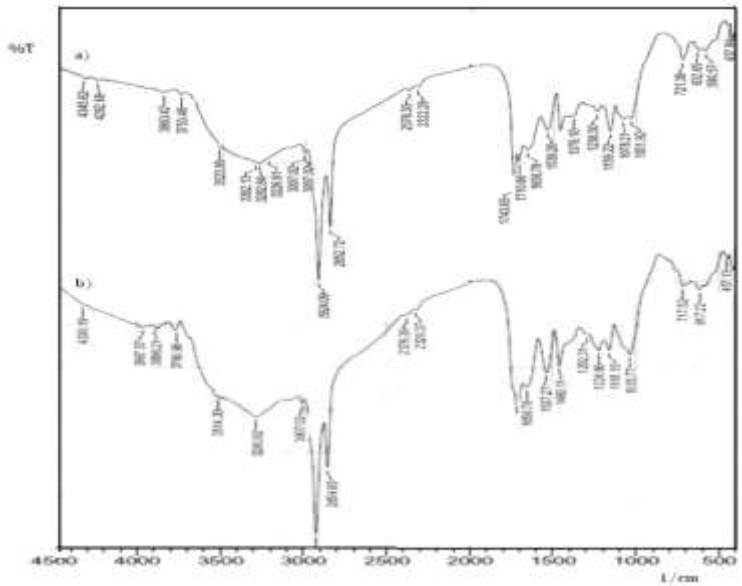

Fig. 5 -Intra-particle diffusion model

ISSN: 2277-9655
Impact Factor: 4.116
CODEN: IJESS7

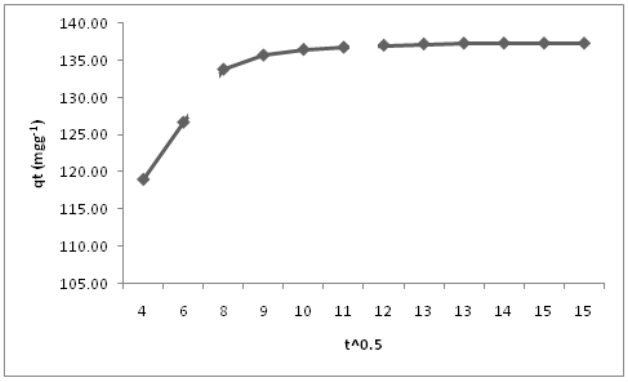

Fig. 6- Liquid film diffusion model

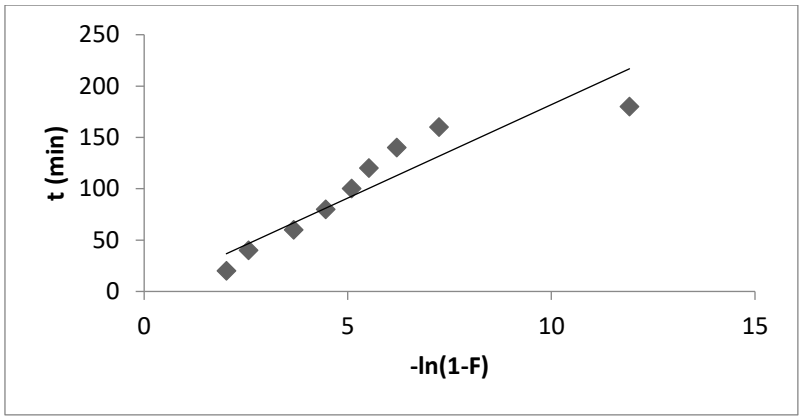

Fig. 7-Sorption desorption cycles for RO 13 dye

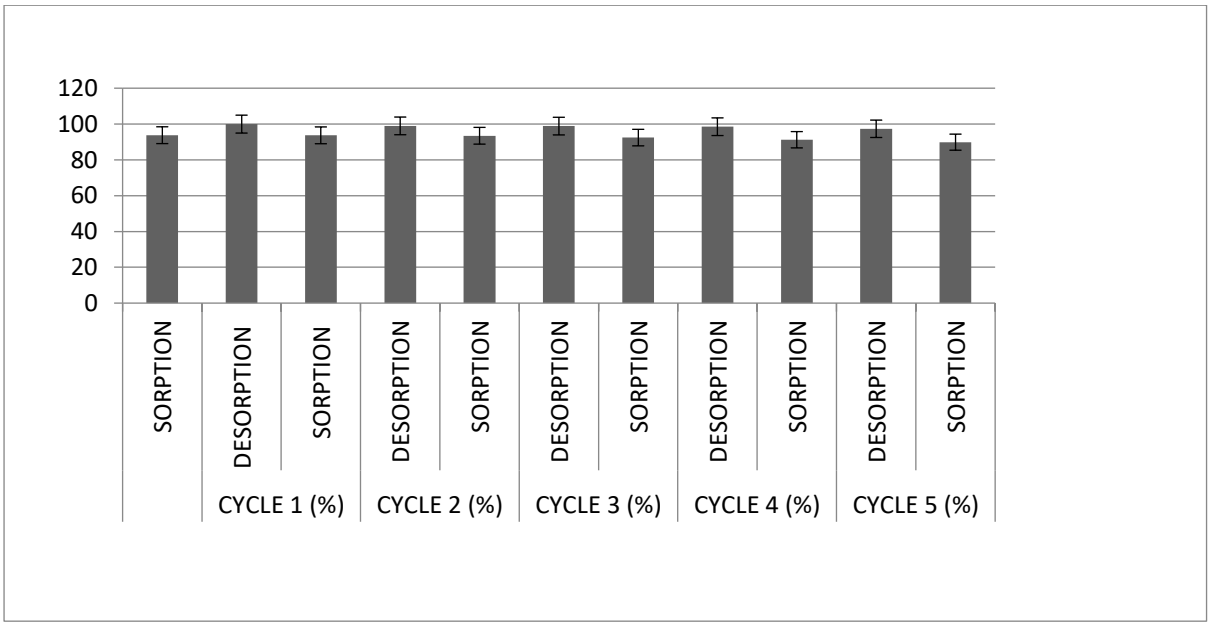

Fig. 8- Molecular dimensions of RO13 using ACD/LABS version 10.0

ISSN: 2277-9655
Impact Factor: 4.116
CODEN: IJESS7

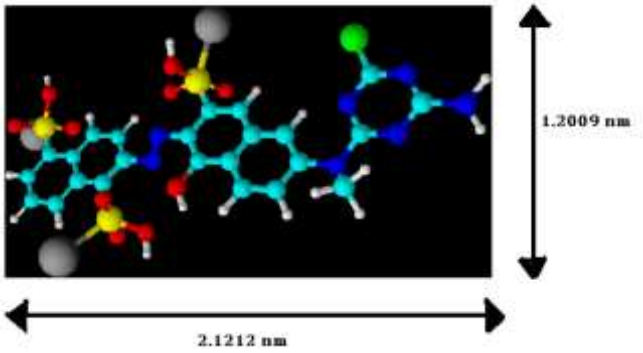

Table 1- Isotherm parameters and error analysis for adsorption of RO 13 on R. arrhizus

Langmuir		Freundlich		Temkin		Dubinin-Radushkovich	
$q_{e,exp}$ (mgg^{-1})	137.27	$q_{e,\ exp}$ ($mg\ g^{-1}$)	137.27	$q_{e,\ exp}$ ($mg\ g^{-1}$)	137.27	$q_{e,\ exp}$ (mgg^{-1})	137.27
$q_{e,\ cal}$ ($mg\ g^{-1}$)	137.09	$q_{e,\ cal}$ ($mg\ g^{-1}$)	137.84	$q_{e,\ cal}$ ($mg\ g^{-1}$)	137.09	$q_{e,\ cal}$ (mgg^{-1})	151.47
K_L (Lmg^{-1})	1.14	K_F	160.77	B ($J\ mol^{-1}$)	12.44	B_D ($mg\ g^{-1}$)	$5.0*10^{-7}$
R_L	0.007	n	10.42	A_T (Lg^{-1})	157.6	E ($KJmol^{-1}$)	1.00
				b	19.26		
R^2	0.998		0.97		0.975		0.823
SSE	0.0324		0.3249		0.2025		201.64
SAE	0.18		0.57		0.45		14.2
ARE	$1.31*10^{-3}$		$4.152*10^{-3}$		$3.278*10^{-3}$		0.103
HYBRID	$2.36*10^{-4}$		$2.367*10^{-3}$		$1.475*10^{-3}$		1.468
MPSD	$1.72*10^{-6}$		$1.72*10^{-5}$		$1.074*10^{-5}$		0.010

Table 2- Kinetic parameters and error analysis for adsorption of RO 13 on R. arrhizus

First Order		Second Order		Elovich		Intra particle		Liquid film diffusion	
$q_{e,\ exp}$ (mgg^{-1})	137.27	$q_{e,\ exp}$ (mgg^{-1})	137.27	$q_{e,\ exp}$ ($mg\ g^{-1}$)	137.27	$q_{e,\ exp}$ (mgg^{-1})	137.27	$q_{e,\ exp}$ (mgg^{-1})	137.27
$q_{e,\ calc}$ (mgg^{-1})	1.27	$q_{e,\ calc}$ (mgg^{-1})	138.62	$q_{e,\ calc}$ (mgg^{-1})	146.27	$q_{e,\ calc}$ (mgg^{-1})	140.97	$q_{e,\ calc}$ (mgg^{-1})	147.18
k_1 (min^{-1})	0.015	k_2 ($gmg^{-1}min^{-1}$)	0.6863	α ($mgg^{-1}min$)	131162	k_{id} ($mgg^{-1}min^{-1/2}$)	3.888	F	1.0001
				β (gmg^{-1})	0.104	C (mgg^{-1})	102	k_{fd} ($Lmin^{-1}$)	0.0456
R^2	0.989		0.999		0.93		0.976		0.92
SSE	18496		1.822		81		13.69		98.21
SAE	136		1.35		9.0		3.7		9.91
ARE	0.99		$9.8*10^{-3}$		$6.55*10^{-2}$		$2.69*10^{-2}$		$7.21*10^{-2}$

ISSN: 2277-9655
Impact Factor: 4.116
CODEN: IJESS7

HYBRID	134.74	$1.32*10^{-2}$	0.59	$9.97*10^{-2}$	0.71
MPSD	0.981	$9.67*10^{-5}$	$4.29*10^{-3}$	$7.27*10^{-4}$	$5.21*10^{-3}$

REFERENCES

[1] Abirami, S., Srisudha, S., Gunasekaran, P., 2013.Comparative study of chromium biosorption using brown, red , green macro algae. Int. J. Biol. Pharm. Res. 42, 115-129.
[2] Akar,S. T., Akar, T., Çabuk, A., 2009. Decolorization of a textile dye, Reactive Red 198 RR198, by Aspergillus parasiticus fungal biosorbent. Brazilian J. Chem. Eng. 2602,399 – 405.
[3] Aksakal, O., Ucun, H., 2010. Equilibrium, kinetic, thermodynamic studies of the biosorption of textile dye Reactive Red 195 onto Pinus sylvestris L. J. Hazard. Mater. 181, 666–672.
[4] Aksu, Z. , Tezer, S., 2000. Equilibrium , kinetic modeling of biosorption of Remazol Black B by Rhizopus arrhizus in a batch system, effect of temperature. Proc. Biochem. 36,431–439.
[5] Aksu, Z., Donmez, G., 2003. A comparative study on the biosorption characteristics of some yeasts for Remazol Blue reactive dye. Chemosphere 50, 1075–1083.
[6] Allen, S. J., McKay, G., Khader, K. Y. H., (1989). Intraparticle Diffusion of a Basic Dye During Adsorption onto Sphagnum Peat. Environ. Pollut.56, 39-50.
[7] Altaher, H., Khalil, T. E. , Abubeah, R., 2014.The effect of dye chemical structure on adsorption on activated carbon, a comparative study.doi: 10.1111/cote.12086
[8] Ambrósio, S.T., José, C., Vilar, J., Carlos, A., Alves, S., Kaoru, O., Nascimento, A.E., Longo, R.L., Takaki, G.M.C., 2012. A Biosorption isotherm model for the removal of reactive azo dyes by inactivated mycelia of Cunninghamella elegans UCP542. Molecules 17, 452-462.
[9] Arıca, M.Y., Bayramoğlu, G., 2005. Cr(VI) biosorption from aqueous solutions using free , immobilized biomass of Lentinus sajor-caju, preparation: kinetic characterization. Colloid Surface A 253, 203–211.
[10] Aroua, M.K., Leong, S.P.P., Teo, L.Y., Yin, C.Y., Daud, W.M.A.W., 2008. Real-time determination of kinetics of adsorption of lead(II) onto palm shell-based activated carbon using ion selective electrode. Bioresour. Technol. 99, 5786–5792.
[11] Arslan, A.I., Insel, G., Eremektar, G., Germirli, B., Orhond, F., 2006. Effect of textile auxiliaries on the biodegradation of dye house effluent in activated sludge. Chemosphere 62,1549-1557.
[12] Aravind, U.K., George, B., Baburaj, M.S., Thomas, S., Thomas, A. P., Aravindkumar, C.T., 2010. Treatment of industrial effluents using polyelectrolyte membranes. Desalination 252, 27–32.
[13] Asgher, M., Bhatti, H. N., 2012.Evaluation of thermodynamics: effect of chemical treatments on sorption potential of Citrus waste biomass for removal of anionic dyes from aqueous solutions. Ecol. Eng.38, 79–85.
[14] Bayramoglu, G., Arica, Y.M., 2006. Biosorption of benzidine based textile dyes “Direct Blue 1 , Direct Red 128” using native , heat treated biomass of Trametes versicolor. J. Hazard. Mat. 143, 135–143.
[15] Binupriya, R., Sathishkumar, M., Kavitha, D., Swaminathan, K., Yun, S-E. , Mun, S-P., 2007.Experimental and Isothermal Studies on Sorption of Congo Red by Modified Mycelial Biomass of Woodrotting Fungus. Clean 352,143 – 150.
[16] Boyd, G.E., Adamson, A.W. , Myers Jr., L.S., 1947. The Exchange Adsorption of Ions from Aqueous Solutions by Organic Zeolites (II) Kinetics. J. American Chem. Society. 69, 2836-2848.
[17] Brdar, M. M., Takači, A. A., Šćiban, M. B., Rakić, D. Z., 2012. Isotherms for the adsorption of CuII onto lignin – comparison of linear, non-linear methods. Hem. Ind. 66 (4),497–503.
[18] Bulut, E., O¨ zacar, M., S¸ engil, ˙I. A., 2008. Equilibrium , kinetic data , process design for adsorption of Congo Red onto bentonite. J. Hazard. Mater. 154,613–622.
[19] Cardoso, N.F., Lima, E.C., Pinto, I.S., Amavisca, C.V., Royer, B., Pinto, R.B., Alencar, W.S., Pereira, S.F.P., 2010. Application of cupuassu shell as biosorbent for the removal of textile dyes from aqueous solution. J. Environ. Manage. 92,1237-1247.
[20] Chen, B-Y., Chen, S -Y., Chang. J-S., 2005. Immobilized cell fixed-bed bioreactor for wastewater decolorization. Process Biochem. 40, 3434–3440.
[21] Chen, Z., Deng, H., Chen, C., Yang, Y. , Xu, H., 2014.Biosorption of malachite green from aqueous Biosorption of malachite green from aqueous solutions by Pleurotus ostreatus using Taguchi method. J. Environ. Health Sci. Eng. 12,63. http,//www.ijehse.com/content/12/1/63.
[22] Crini, G. , Badot, P., 2008.Application of chitosan, a natural aminopolysaccharide, for dye removal from aqueous solutions by adsorption processes using batch studies, A review of recent literature. Prog. Polym. Sci. 33,399–447.

ISSN: 2277-9655
Impact Factor: 4.116
CODEN: IJESS7

[23] Dhananjay Kumar, Pey, L. K. , Gaur, J.P., 2010. Evaluation of various isotherm models and metal sorption potential of cyanobacterial mats in single and multi-metal systems. Colloids , Surfaces B, Biointerfaces 81, 476–485.
[24] Dubinin, M.M., Radushkevich, L.V., 1947. The equation of the characteristic curve of the activated charcoal. Proc. Acad. Sci. USSR Phys. Chem. Sect. 55, 331–337.
[25] Erden, E., Kaymaz, Y.,Pazarlioglu, N. K., 2011. Biosorption kinetics of a direct azo dye Sirius Blue K-CFN by Trametes versicolor. E. J. Biotechnol. 142. http,//dx.doi.org/10.2225/vol14-issue2-fulltext-8 – 2011
[26] Filipkowska, U., Klimiuk, E., Kuczajowska-Zadrożna, M., Kuś, S., 2004.The Removal of reactive dyes from binary mixtures using chitin. Pol J Environ Stud 13 6, 653-661.
[27] Fiorentin, L. D., Trigueros, D. E.G., Módenes, A. N., Espinoza-Quinones, F. R., Pereira, N. C., Barros, S.T.D. , Santos, O. A.A., 2010. Biosorption of reactive blue 5G dye onto drying orange bagasse in batch system: Kinetic , equilibrium modeling. Chem. Eng. J. 163, 68–77.
[28] Florence, J.A.K., Gomathi, T., Thenmozhi, N., Sudha, P. N., 2015. Adsorption study: Removal of nickel ions using Kenaf fiber/chitosan biosorbent. J. Chem. Pharm. Res.75, 410-422.
[29] Foo, K.Y. , Hameed, B.H., 2010. Insights into the modeling of adsorption isotherm systems. Chem. Eng. J. 156,2–10.
[30] Freundlich, H.M.F., 1906.Over the adsorption in solution. J. Phys. Chem. 57,385–471.
[31] Giles, C.H., Smith, D. , Huitson, A., 1974. A General Treatment, Classification of the Solute Adsorption Isotherm. Colloid Interface Sci. 47 (3), 755 - 765.
[32] Geethakarthi, A., Phanikumar, B. R., 2011. Adsorption of reactive dyes from aqueous solutions by tannery sludge developed activated carbon, Kinetic and equilibrium studies. Int. J. Environ. Sci. Tech. 8 (3),561-570.
[33] Gnanasambam, R., Protor, A., 2008. Determination of pectin degree of esterification by diffuse reflectance Fourier Transform Infrared Spectroscopy [J]. Food Chem 68, 327−332.
[34] Guibal, E., Milot, C., Tobin, J.M., 1998. Metal-Anion Sorption by Chitosan Beads, Equilibrium and Kinetic Studies. Ind. Eng. Chem. Res. 37, 1454-1463.
[35] Gupta, V.K., Srivastava, S.K., Tyagi, R., 2000. Design parameters for the treatment of phenolic wastes by carbon columns obtained from fertilizer waste material. Water Res. 34, 1543–1550.
[36] Ho, Y.S., McKay, G., 2000. Correlative biosorption equilibria model for a binary batch system. Chem Eng Sci 55, 817-825.
[37] Ho, Y. S., 2004. Citation review of Lagergren kinetic rate equation on adsorption reactions. Scientometrics 59,171–177.
[38] Ho, Y.S. , McKay, G., 2002. Application of Kinetic Models to the Sorption of Copper(II) on to Peat. Adsorption Sci. Technol. 208,797-815.
[39] Ho, Y.S., McKay, G., 1998. A comparison of chemisorption kinetic models applied to pollutant removal on various sorbents. Trans. Icheme 76 B, 332–339.
[40] Ilhan, S., Iscen, C. F., Caner, N., Kiran, I., 2008.Biosorption potential of dried Penicillium restrictum for Reactive Orange 122, isotherm, kinetic, thermodynamic studies. J Chem Technol Biotechnol 83,569–575.
[41] Itodo, A.U., Itodo, H.U., 2010. Sorption Energies Estimation Using Dubinin-Radushkevich ,Temkin Adsorption Isotherms. Life Sci. J. 74,31-39.
[42] Juang, R.S., Tseng, R.L., Wu, F.C., Lee, S.H., 1997.Adsorption behavior of reactive dyes from aqueous solutions on chitosan. J Chem Tech Biotechnol 70,391–9.
[43] Kadirvelu, K., Kavipriya, M., Karthika, C., Radhika, M., Vennilamani, N., Pattabhi, S., 2003. Utilization of various agricultural wastes for activated carbon preparation, application for the removal of dyes and metal ions from aqueous solutions. Biores. Technol. 87,129–132.
[44] Kapoor, A., Viraraghavan, T., 1997. Heavy metal biosorption sites in Aspergillus niger. Bioresour. Technol. 61, 221–227.
[45] Lagergren, S., 1898.About the Theory of So- Called Adsorption of Soluble Substances. Kunglia Svenska Vetenskapsakademiens. H, lingar, B, 244, 1-39.
[46] Liu, Y., Liu, Y.-J., 2008. Biosorption isotherms, kinetics and thermodynamics. Separation Purification Technol. 61, 229–242.
[47] Mathur, N., Bhatnagar, P., 2007. Mutagenicity assessment of textile dyes from Sanganer Rajasthan. J. Environ. Biol. 281, 123-126.
[48] McKay, G., Ho, Y. S. , Ng,J. C. Y., 1999. Biosorption of copper from wastewaters, A review. Sep. Purif. Meth. 28, 87 – 125.

[49] Murugesan, K., 2003. Bioremediation of paper, pulp mill effluents. Ind. J. Exp. Biol. 4111,1239-1248.
[50] Nakagawa, K., Namba, A., Mukai, S., Tamon, H., Ariyadejwanich, P., Tanthapanichakoon, W., 2004. Adsorption of phenol, reactive dye from aqueous solution on activated carbons derived from solid wastes. Water Res. 38, 1791-8.
[51] Naja, C., Mustin, C., Volesky, B., Berthelin, J., 2005. A high-resolution titrator: A new approach to studying binding sites of microbial biosorbents. Water Res. 39, 579–588.
[52] Namasivayam, C., Kavitha, D., 2002. Removal of congo red from water by adsorption onto activated carbon prepared from coir pith, an agricultural solid waste. Dyes Pigments 54, 47–58.
[53] Netpradit, S., Thiravetyan, P., Towprayoon, S., 2004. Application of ‘‘waste’’ metal hydroxide sludge for adsorption of azo reactive dyes. Water Res. 37,763–772.
[54] Oladoja, N. A., Aboluwoye, C. O. , Oladimeji, Y. B., 2008. Kinetics , Isotherm Studies on Methylene Blue Adsorption onto Ground Palm Kernel Coat. Turkish J. Eng. Env. Sci.32 , 303 – 312.
[55] Palanisamy, P. N., Agalya, A. , Sivakumar, P., 2013. Equilibrium uptake, sorption dynamics for the removal of reactive dyes from aqueous solution using activated carbon prepared from Euphorbia tirucalli L wood. Indian J. Chem. Technol. 245-251.
[56] Parvathi, K., Nagendran, R., Nareshkumar, R., 2007. Lead biosorption onto waste beer yeast by-product, a means to decontaminate effluent generated from battery manufacturing industry. Electron. J. Biotechnol. 101, 92-105.
[57] Patel, R., Sumathi, S., 2008. Kinetic , equilibrium studies on the biosorption of reactive black 5 dye by Aspergillus foetidus. Biores. Technol. 99,51–58.
[58] Piccin, J. S., Dotto, G. L. , Pinto, L. A. A., 2011.Adsorption isotherms , thermochemical data of FD&C Red N° 40 binding by chitosan. Braz. J. Chem. Eng. 28 (2), 295 – 304.
[59] Qiu, H., Lu, L.V., Pan, Zhang, B.-cai, Zhang, Q.-jian, Ming W. , Zhang, Q.-xing, 2009.Critical review in adsorption kinetic models. J Zhejiang Univ Sci A 105,716-724.
[60] Ramrakhiani, L., Majumder, R., Khowala, S., 2011. Removal of hexavalent chromium by heat inactivated fungal biomass of Termitomyces clypeatus, Surface characterization, mechanism of biosorption. Chem. Eng. J. 171,1060– 1068.
[61] Russo, M. E., Marzocchella, A., Olivieri, G., Prigione, V., Salatino, P., Tigini, V., Varese, G.C., 2009. Pierucci, S. ed., ICheaP-9, 9th International Conference on Chemical , Process Engineering. AIDIC, Milano 10-13 May 2009, Rome, Italy pp 1071-1076 Chemical Engineering Transactions, 17. ISBN, 9788895608013.
[62] Sağ, Y., Aktay, Y., 2002. Kinetic studies on sorption of Cr (VI) , Cu (II) ions by chitin, chitosan , Rhizopus arrhizus. Biochem. Eng. J. 122,143-153. doi,10.1016/S1369-703X0200068-2.
[63] Saraf, S., Vaidya, V. K., 2015.Statistical optimization of biosorption of Reactive Orange 13 by dead biosorbent of Rhizopus arrhizus NCIM 997 using response surface methodology. Int J Ind Chem 6, 93–104.
[64] Shroff, K. A., Vaidya V. K., 2011. Kinetics, equilibrium studies on biosorption of nickel from aqueous solution by dead fungal biomass of Mucor hiemalis. Chem. Eng. J. 171, 1234–1245.
[65] Shroff, K. A., Vaidya, V. K., 2012.Effect of pre-treatments on the biosorption of Chromium VI ions by the dead biomass of Rhizopus arrhizus. J. Chem. Technol. Biotechnol.87, 294-304.
[66] Skult, F., 2009.The biosorption behavior of inactive Aspergillus niger modified by autoclaving in treating dye wastewater. Thesis, Undergraduate Student Research Program, Lund University.
[67] Smith, B., 1999. Infrared Spectral Interpretation: A Systematic Approach. CRC Press, Boca Raton.
[68] Sulaymon, A. H. , Abood,W. M. 2013.Competitive Adsorption of Three Reactive Dyes by Activated Carbon. J. Eng. 19 (6), 655-667.
[69] Swamy, J., 1998. The biodecoloration of textile dyes by the white rot fungus Trametes versicolor. Thesis, department of chemical engineering, Queen’s university, Canada.
[70] Swamy, J., Ramsay, J. A., 1998. The evaluation of white rot fungi in the decoloration of textile dyes. Enzyme , Microbial Technol. 24,130–137.
[71] Thompson, G., Swain, J., Kay, M., Forster, C.F., 2001. The treatment of pulp, paper mill effluent, a review, Bioresour. Technol. 77, 275–286.
[72] Tempkin, M.I., Pyzhev, V., 1940.Kinetics of ammonia synthesis on promoted iron catalyst. Acta Phys. Chim. USSR 12,327–356.
[73] Teng, H., Hsieh, C., 1999.Activation energy for oxygen chemisorption on carbon at low temperatures. Ind. Eng. Chem. Res. 381,292 -297.
[74] Tunali, S., Kiran, I. , Akar, T., 2005. Chromium VI biosorption characteristics of Neurospora crassa fungal biomass. Miner. Eng. 18,681–689.

ISSN: 2277-9655
Impact Factor: 4.116
CODEN: IJESS7

[75] Tsezos, M., 1983.The role of chitin in uranium adsorption by Rhizopus arrhizus. Biotechnol Bioeng 25, 2025-2040.
[76] Uzun, İ., 2006. Kinetics of the adsorption of reactive dyes by chitosan. Dyes Pigments 70, 76-83.
[77] Vasanth Kumar, K., Porkodi, K., 2007.Mass transfer, kinetics and equilibrium studies for the biosorption of methylene blue using Paspalum notatum. J. Hazard. Mater. 146, 214–226.
[78] Volesky, B., 2007. Biosorption and me. Water Res. 41, 4017-4029.
[79] Walker, G.M., Weatherley, L.R., 2000. Textile wastewater treatment using granular activated carbon adsorption in fixed beds. Sep. Sci. Technol. 39,1329–1341.
[80] Weber, W. J. Jr., Morris, J. C., 1963.Kinetics of adsorption on carbon from solution. J. Sanit. Eng. Div. ASCE. 89,31-59.
[81] Yang, Y., Li, Z., Wang, G., Zhao, X.-P., Crowley, D.E., Zhao, Y.-H., 2012. Computational identification, analysis of the key biosorbent characteristics for the biosorption process of Reactive Black 5 onto Fungal Biosorbent. PLOS one 7 (3). Doi: 10.1371/journal.pone.0033551.
[82] Zille, A., 2005, Laccase reactions for textile applications. Dissertation, the University of Minho, Italy.